

TANDEM MASS SPECTROMETRY REVEALS THE QUATERNARY ORGANIZATION OF MACROMOLECULAR ASSEMBLIES

*Justin L.P. Benesch, J. Andrew Aquilina¹, Brandon T. Ruotolo, Frank Sobott², Carol V. Robinson **

Department of Chemistry, University of Cambridge, Lensfield Road, Cambridge, CB2 1EW, U.K

¹ Present Address: School of Biological Sciences, University of Wollongong, Northfields Avenue, Wollongong, NSW 2522, Australia

² Present Address: Structural Genomics Consortium, University of Oxford, Botnar Research Centre, Oxford, OX3 7LD, UK

* Corresponding Author: Tel: +44 1223 763846, Fax: +44 1223 763843, Email: cvr24@cam.ac.uk

Running Title: Tandem MS of Macromolecular Assemblies

SUMMARY

The application of mass spectrometry (MS) to the study of progressively larger and more complex macromolecular assemblies is proving increasingly useful for structural biologists. The scope of this approach has recently been widened through the application of a tandem MS procedure. This two-step technique involves the selection of specific assemblies in the gas phase, and inducing their dissociation through collisions with argon atoms. Here we investigate the mechanism of this process and show that dissociation of subunits from a macromolecular assembly follows a sequential pathway, with the partitioning of charge between the dissociation products governed primarily by their relative surface areas. Using this basis of understanding, we highlight differences in the dissociation pathways of three related macromolecular assemblies and show how these are a direct consequence of changes in both local and global oligomeric organization.

INTRODUCTION

Various methods are used to achieve the principal goal of structural biology, namely determining the organization of biological macromolecular assemblies. Electrospray mass spectrometry (ES-MS) is rapidly becoming an attractive complementary methodology to traditional approaches such as X-ray crystallography, nuclear magnetic resonance, and electron microscopy [1, 2]. When used in isolation ES-MS is able to determine the stoichiometry of protein complexes, but when used in conjunction with other approaches new insight into complexes and sub-complexes can often be obtained. For example MS has provided key information regarding the overall stoichiometry of assemblies, enabling fitting of high resolution structures to electron density maps [3, 4]. Furthermore, the applicability of MS to massive and highly complex molecular machines is highlighted by an MS study of intact ribosomes which defined the copy number of associated protein complexes [5]. Therefore, in the post-genomic era MS is not only crucial in analyzing gene products [6], but is also becoming increasingly valuable in studying the nature of their interactions.

Though spectra can be recorded for complexes in excess of 1MDa, they are still, however, much smaller than the species in excess of 100MDa which have been transmitted into the gas phase by ES [7]. A major reason why such large ions cannot be successfully measured by MS alone is due to the nature of the ES process whereby such ions carry a large and, moreover, variable amount of charge. Consequently there is only very small separation between these adjacent charge states¹. This represents

¹ The predicted charge z , where m is the assembly mass is given by the following relationship: $z \approx 0.078 \times \sqrt{m}$ [8]. de la Mora, J.F. (2000). Electrospray ionization of large multiply charged species proceeds via Dole's charged residue mechanism. *Anal. Chim. Acta* 406, 93-104.]. For example, a 100MDa complex would therefore be expected to carry approximately 780 charges. This 780+ charge state hence would appear at $128206m/z$, and the adjacent 781+ charge state at $128042m/z$, a difference of $164m/z$. Such separation presents a

a major challenge if the mass range of species amenable to study by MS is to continue to increase, particularly as issues of protein purity become more important as the stoichiometry of a macromolecular complex increases^{II}. Further compounding these difficulties is the tendency of many biologically important assemblies to be naturally heterogeneous and polydisperse. To address this problem we have recently developed a tandem MS (MS/MS) approach which employs the technique of collision-induced dissociation (CID) to dissociate specific macromolecular species, selected via their mass to charge (m/z) ratios [10]. We reasoned that an MS/MS approach would allow us the ability to select different regions of mass spectra obtained for heterogeneous assemblies, and consequently enable us to probe the stoichiometry of the interacting subunits. Moreover, dissociating the assembly would act to reduce the charge on the oligomeric species involved, and thereby distribute the ion signal over a much wider m/z range than would be achieved by one-dimensional MS. This has provided a means of defining species which could not be adequately characterized by traditional structural approaches or by MS alone, and has consequently opened a new avenue in the structural biology of macromolecular assemblies [11].

The separation via charge reduction that can be achieved through such an approach arises from the unique ‘asymmetric’ nature of the dissociation of multimeric protein complexes. This phenomenon was recognized when an early study showed that activation of tetrameric proteins in the mass spectrometer

significant challenge as the spectra of intact noncovalent complexes is limited by the extent of desolvation that is possible without disruption of the complex [9. Sobott, F., and Robinson, C.V. (2004). Characterising electrosprayed biomolecules using tandem-MS - the noncovalent GroEL chaperonin assembly. *Int. J. Mass Spectrom.* 236, 25-32.].

^{II} The probability of an oligomer of n subunits being composed entirely of pure monomer (P_O) is dependent on monomer purity (P_M) according to the following equation: $P_O (\%) = [P_M (\%)^n] / [100^{n-1}]$. An oligomer composed of 10 subunits, with a monomeric purity of

results in the formation of complementary monomeric and trimeric products, with the monomers claiming a much larger proportion of the charge than might be expected [12]. Subsequent studies have shown that this asymmetric separation of mass and charge into highly charged monomers and lowly charged ‘stripped oligomers’ occurs in the gas-phase dissociation of numerous protein complexes [9, 12-21]. The basic pathway of protein assembly dissociation in the mass spectrometer can therefore be described as follows:

$$n^q \rightarrow [n-1]^{q-x} + m^x$$

where n is the number of subunits in the oligomer, q is the number of charges on the oligomer and x is the average charge carried by a monomer m . Moreover, it has been shown that this process can occur such that several monomers can be removed from an oligomer [11, 22-24], though the pathway of this multiple loss of subunits is not known. The result of these asymmetric dissociation events is that the resulting stripped oligomers are of much lower charge state than the parent oligomers. Consequently the separation between adjacent charge states is vastly improved, and the possibility that individual species can be readily identified is greatly increased [11]. This approach has aided the characterization of species across many fields of structural biology, including ribosomal sub-complexes [5], membrane proteins [25], protein-degradation machinery [26], and molecular chaperones [27-29].

Though the use of this approach is already providing valuable insight into the organization of macromolecular assemblies and their components, the mechanism of dissociation of multimeric assemblies remains the matter of some debate, and consequently the detailed application of this technique remains compromised. An early study on the gas phase dissociation of small noncovalent

90% would result in 35% pure oligomer, whereas if the oligomer was composed of 100 subunits, the oligomeric purity would drop to $2.7 \times 10^{-3}\%$.

protein complexes speculated that “dissociation of the [oligomer] may occur by a Coulombically driven process in which a monomer becomes ‘unraveled’ and ejected from the aggregate with a disproportionately large share of the charge” [12]. A large entropy gain during the dissociative transition-state observed during the dissociation of a small pentameric protein complex [13], and investigations into the effect of flexibility within the components of the protein assembly [15, 16] provide evidence for this to be the case. It remains to be seen whether mechanistic details extrapolated from studies of smaller protein assemblies will translate to an understanding of the dissociation of larger systems. Therefore, it is of paramount importance for the continuing development of MS in the field of structural biology that the characteristics of the CID of a range of large macromolecular assemblies is examined, such that a proper basis for understanding can be achieved.

We report here detailed investigations into the dissociation of three proteins which form large noncovalent complexes: *Ta*HSP16.9 from wheat, which is composed of 12 subunits [30]; *Mj*HSP16.5 from *Methanococcus jannashii*, which is composed of 24 subunits [31]; and bovine α B-crystallin, which forms a polydisperse assembly centered around 28 subunits [11]. MS/MS experiments performed on these proteins result in their dissociation into monomers and various stripped oligomers. We show that this proceeds in a sequential manner with the charges redistributed in a Coulombically favourable fashion determined by their relative surface areas. This characteristic causes effective charge reduction, and acts to increase peak separation by distributing the resulting spectrum over a broad m/z range. The power of this approach is exemplified in the MS/MS of α B-crystallin, where the stoichiometry of all the component oligomers can be determined enabling a global description of the oligomeric organization, despite an extreme level of heterogeneity. Furthermore we show how, through a detailed examination of dissociation pathways, valuable insight into the local organization of macromolecular assemblies and their subunit interactions can be gained.

RESULTS AND DISCUSSION

A common dissociation pathway for macromolecular assemblies

Mass spectra of the small heat shock proteins (sHSPs) *Ta*HSP16.9 and *Mj*HSP16.5, introduced using a miniaturized version of ES known as nanoES [32], are shown in figure 1A and B. In each case a single species is observed, corresponding to masses of 200790Da, and 395107Da respectively. From comparison with the masses calculated from the polypeptide sequences, we can conclude that *Ta*HSP16.9 and *Mj*HSP16.5 form monodisperse 12mers and 24mers respectively, and that these native stoichiometries [30, 31] can be preserved in the gas phase of the mass spectrometer without dissociation.

When the accelerating voltages and vacuum are raised in the source region of the mass spectrometer, thereby increasing the ions' acceleration between collisions with surrounding gas molecules, a spectrum of *Mj*HSP16.5 shows peaks corresponding to monomers at low m/z , and stripped oligomers (23mers and 22mers) at high m/z (Fig. 1C). Similarly activation for *Ta*HSP16.9 results in the formation of monomers and 11mers [33]. This technique is known as 'in-source' CID. Alternatively, ion activation can also be achieved downstream in the spectrometer by accelerating the ions into a gas-filled collision cell. A spectrum obtained when *Mj*HSP16.5 is dissociated in this way is shown in figure 1C. Again monomers, 23mers and 22mers are observed. This demonstrates that the products, and hence likely the mechanism, of dissociation of these large protein complexes is essentially the same despite the activation occurring at different stages of the mass spectrometer. As such, the mechanistic conclusions we draw below apply to dissociation performed in both the source region or collision cell.

Though the two proteins have different overall architecture (*Ta*HSP16.9 is disc-shaped [30], *Mj*HSP16.5 is spherical [31]), they are both composed of dimeric ‘building blocks’ [34]. Heating *Ta*HSP16.9 in solution leads to the observation of these dimers [33], and subunit exchange experiments monitored by mass spectrometry indicate that the reaction proceeds via loss of dimers from the oligomeric complex [35]. The dissociation experiments presented here, showing the loss of monomers, are in direct contrast to this (Fig. 1), demonstrating that while dissociation may exhibit the same characteristics, irrespective of where activation occurs in the instrument, it follows a fundamentally different pathway in the gas phase to that which takes place in solution. One of the main advantages of this dissociation is, however, that the masses of the monomers, oligomers, and stripped oligomers are all measured within the same experiment. Therefore it is possible to determine the overall stoichiometry, even in cases where the sequence of the component monomeric subunit is unknown.

Sequential removal of subunits allows characterization of oligomeric species

To investigate the mechanism of the dissociation process, we performed MS/MS experiments wherein a particular charge state of a species is selected and dissociated. The dissociation pathway of the *Ta*HSP16.9 12mer is shown in figure 2. At the lowest collision energies, the 12mers remain intact. Increasing the accelerating voltage results in the formation of monomer and stripped complexes comprising 11subunits. At the highest collision energies 10mers are also observed (Fig. 2A). These 10mers are only formed once the accelerating voltage reaches 120V. At this point 12mers are no longer observed, and the relative abundance of 11mers starts to decay, having reached a maximum (Fig. 2B). Therefore the 10mers must be formed from the 11mers, which have, in turn, been formed from the 12mers. This indicates that this process is occurring in a sequential manner (Fig. 2C). Similarly the loss of multiple subunits is also observed for the dissociation of the *Mj*HSP16.5 24mers (Fig. 3). The onset of dissociation into monomers and 23mers occurs at approximately 70V, and, at slightly higher

collision energies, 22mers are formed. At the highest collision energies 21mers are also observed, showing that in this case as many as three subunits can be removed from the parent oligomer (Fig. 3A). The results presented here clearly show that multiple loss of subunits during CID, is a sequential process rather than a concerted one.

The spectra of the stripped oligomers show that despite the fact that very narrow m/z ranges were selected from the mass spectra (typically isolation windows 30 m/z wide) the resulting MS/MS spectra are distributed over much wider m/z ranges (12000 and 18000 m/z respectively) (Fig. 2A and 3A). The sequential loss of highly charged subunits results in the charge-reduction of the oligomeric components, and subsequently the separation between adjacent peaks is greatly increased. Whereas adjacent peaks corresponding to the intact 24mer of *MjHSP16.5* are separated by $\sim 190m/z$ (Fig. 1C), the removal of successive monomers results in separations of $\sim 360m/z$, $\sim 790m/z$, $\sim 1650m/z$ (for 23mers, 22mers and 21mers, respectively). The potential of this characteristic is exemplified by performing dissociation on another sHSP, α B-crystallin. Unlike its monodisperse plant and bacterial counterparts described above, this protein forms a polydisperse assembly centered around 28 subunits [11]. An MS spectrum of this protein features overlapping charge state series from 6000 to 14000 m/z corresponding to all the different contributing components of this polydisperse assembly (Fig. 4A). We performed MS/MS on the peak corresponding to an overlap of all the oligomers, each carrying twice as many charges as subunits (10040 m/z) [11]. As the accelerating voltage is increased, up to three monomers can be removed from the different oligomers (Fig. 4B). The peaks corresponding to the charge states of the variously stripped oligomers originating from a parent 28mer⁵⁶⁺ were monitored, and show a sequential reaction pathway, similar to that of *MjHSP16.5* (Fig. 4C). The result of the charge reduction effected by this consecutive loss of subunits is that whereas peaks could not be

sufficiently separated by MS alone (Fig. 4A), after stripping of highly charged subunits, individual assemblies can be resolved (Fig. 4B inset), and consequently their relative populations quantified [11].

Such charge reduction is increasingly important as progressively larger and more complex species are studied by means of MS. As well as distributing the signal over a wider m/z range, the peak width also decreases upon dissociation, most likely as a result of removal of adducted buffer ions and water molecules [9]. This further improves the likelihood of resolving individual species. Moreover, the demonstration that the pathway of the loss of multiple subunits is sequential, paves the way for detailed use of this approach to probe the arrangement of components within macromolecular assemblies [28, 36].

Structural information from charge partitioning during dissociation

In the first dissociation steps of the two monodisperse assemblies (*TaHSP16.9* and *MjHSP16.5*) 46% and 29% of the charge is apportioned to the dissociated monomers respectively. This is a surprisingly large proportion of the charge since the individual subunits comprise only 8.3% and 4.2% of the total mass respectively (Table 1). In other words, during dissociation there is a large asymmetry in the charge partitioning to the subunits that are expelled, relative to their mass. However, as the charges on gas-phase proteins are more likely to be found on surface of the ion, rather than buried within the molecule, analyzing the dissociation patterns with respect to surface area rather than mass (or volume) is perhaps more appropriate [37, 38]. Therefore, we estimated the surface areas of both the stripped oligomers and the monomers that result from this dissociation process. These estimated surface areas are for monomers in an unfolded state, as previous studies have shown this to be their likely conformation during CID [13, 15, 16] (Table 1).

These results show that the surface areas (~40% and ~30%) of the two unfolded monomers from *TaHSP16.9* and *MjHSP16.5* are closely similar to values for charge partitioning to the monomer detailed above (46% and 29%). Moreover the results of all subsequent calculations show that the partitioning of charge between monomers and stripped oligomers closely follows the ratios of their surface areas. In other words, the surface area charge density is constant over the two product ions. This means that, while dissociation is asymmetric with respect to the mass of the ions, it is symmetric with respect to the surface area of the ions. Furthermore, because of the unfolding of the ejected monomer, the total surface area of the products is projected to be larger than that of the parent oligomer. Consequently the surface area charge density decreases with removal of monomers such that the whole process is Coulombically favourable. Therefore we suggest that the main driving force behind the dissociation process for large non-covalent protein-protein complexes is the enthalpic stabilization resulting from a minimization of Coulombic repulsion.

This detailed knowledge of the mechanism at work in the CID of large protein complex ions can allow for extrapolations of ion surface area from charge partitioning ratios. As the surface area charge density is constant over the products, we can, by measuring the partitioning of charge and estimating the surface area of an unfolded monomer, calculate the surface area of the stripped oligomers with the following relationship:

$$Z_{(SO)} / SA_{(SO)} = Z_{(M)} / SA_{(M)} \quad \text{and therefore} \quad SA_{(SO)} = SA_{(M)} Z_{(SO)} / Z_{(M)}$$

where Z is charge, SA is surface area, and the subscripts SO and M refer to stripped oligomers and monomers respectively. This value could then be applied to estimate the surface area of the parent oligomer. This approach, and others based on surface areas [38, 39], may well prove useful in the

future in distinguishing between different possibilities when the structure of a macromolecule is unknown.

A previous investigation into the effect of the conformational flexibility on charge partitioning during dissociation led to the qualitative correlation of ease of protein unfolding with the amount of charge transferred to the monomers [15]. Our proposal that the relative surface areas of products are determinants of charge partitioning is consistent with this finding, as the surface area of a protein is proportional to its degree of unfolding. It is therefore feasible to envisage that charge partitioning data, particularly coupled with an examination of the energetics of activation during CID, may lead to a quantitative assessment of protein folding parameters, and the strength of interactions between subunits.

Interactions between subunits revealed from details of the dissociation pathway

It is interesting to note that loss of a second subunit from stripped *Mj*HSP16.5 oligomers happens at collision energies only slightly higher than those required to detach the first (the difference in voltage between when the maximum amount of 23mer and 22mer are observed is only 20V). This suggests therefore that loss of the second subunit is a relatively easier dissociation process than loss of the first (Fig. 3B). Since it is established that unfolding of the monomer is the crucial step in the dissociation process [13, 15], we can conclude that in the case of *Mj*HSP16.5 unfolding of the second monomer is a facile process compared to unfolding of the first. This observation possibly arises from the dimeric substructure revealed by the crystal structure [31]; once the first monomer of a dimer is removed, the second has fewer interactions to break in order to unfold and detach from the oligomer.

By contrast, the closely related α B-crystallin, if isolated under chemically denaturing conditions, does not contain dimeric substructure; rather, monomers appear to be the basic unit of organization [11]. For this protein, however, the voltage difference between the maxima of the relative abundances of singly and doubly stripped oligomer is 40V, compared to only 20V for *Mj*HSP16.5. This difference is more marked if one takes into account the charge state of the parent ions, thereby comparing the initial kinetic energy of the ions as they enter the collision cell (Fig. 5). From differences in initial kinetic energy of the two species it can be clearly seen that a much smaller increase is required to dissociate the second monomer from the *Mj*HSP16.5 oligomer than from α B-crystallin. We propose that this is a consequence of the dimeric substructure of *Mj*HSP16.5 and the absence of similar interactions in isolated α B-crystallin. This example highlights how tandem MS can be used to elucidate structural information not only in terms of the overall stoichiometry, but also on a local level by probing interactions between neighboring subunits.

SIGNIFICANCE

ES-MS is fast becoming an accepted methodology for establishing the stoichiometry of macromolecular assemblies and is widely applied in conjunction with conventional high resolution structural biology approaches [1]. The capabilities of MS have recently been augmented by the application of tandem MS which acts to remove highly charged monomers from macromolecular assemblies. This not only provides further validation of the stoichiometry of the assembly but, by virtue of charge reduction, also allows characterization of assemblies that cannot be resolved using one-dimensional MS [11]. Here, we have investigated the mechanism of this gas-phase dissociation and established that loss of multiple subunits is a sequential process. We have also ascertained a correlation between the relative surface areas of the products and division of the charge during dissociation. This provides a basis for interpreting tandem MS data and enables elucidation of the global oligomeric organization as well as unambiguous determination of stoichiometry. Furthermore, by careful monitoring of the sequential loss of monomers during the dissociation processes, we have also shown that we can probe the underlying interactions between neighboring subunits allowing us to deduce local structural organization. These experimental observations from the dissociation products and the details of the dissociation pathway, can lead to an array of structural information on both global and local oligomeric levels (Fig. 6).

This study has increased our understanding of the dissociation process as applied to large macromolecular assemblies and highlights the exciting possibility of obtaining important structural information, both locally and globally, for simple homogenous assemblies and complex heterogenous ones. Coupled with the suitability of ES-MS for the study of transient interactions of these species [28,

35, 40], this further highlights the ever-increasing role of MS-based technologies in the analysis of macromolecular complexes.

ACKNOWLEDGMENTS

The authors thank Eman Basha from the Vierling Group (University of Arizona), Lin Lin Ding from the Horwitz Group (Jules Stein Eye Institute, UCLA), and Orval Bateman from the Slingsby Group (Birkbeck College, London) for supplying purified HSP16.9, HSP16.5 and α B-crystallin respectively; and Jane Allison from the Dobson Group (University of Cambridge) for providing PDB files of unfolded proteins. JLPB acknowledges the Engineering and Physical Research Council and Medical Research Council, CVR the Walters Kundert Charitable Trust, and JAA was a Royal Society Howard-Florey Fellow.

EXPERIMENTAL PROCEDURES

Proteins

TaHSP16.9 from wheat and *MjHSP16.5* from *Methanococcus jannashii* were expressed in *E. coli* and purified as described previously [30, 41]. α B-Crystallin was isolated and purified from bovine lenses as described previously [11]. The same buffer exchange procedure was employed for the three proteins: they were loaded onto a Superdex 200HR10/30 gel filtration column (Amersham Pharmacia) and eluted at 0.3mlmin^{-1} with 200mM ammonium acetate at 4°C . The resulting fractions corresponding to the protein oligomers were combined to give final protein concentrations of 0.7mgml^{-1} (*TaHSP16.9*), 1.6mgml^{-1} (*MjHSP16.5*), and 1.2mgml^{-1} (α B-crystallin). These samples were analyzed directly by mass spectrometry.

Nanoelectrospray Mass Spectrometry

Experiments were conducted using a Q-ToF 2TM mass spectrometer (Micromass UK Ltd) which has been modified for high-mass operation [42]. Typically, $2\mu\text{l}$ of solution were electrosprayed from gold-coated glass capillaries prepared in-house. All spectra were calibrated externally using a solution of cesium iodide (100mgml^{-1}), and processed with MassLynx software (Micromass UK Ltd). Spectra are shown here with minimal smoothing, and without background subtraction.

In MS mode, the following instrument parameters were used for the analysis of *TaHSP16.9*/*MjHSP16.5*/ α B-crystallin: capillary voltage 1.65/1.65/1.6kV, cone gas 100Lh^{-1} , sample cone 200V, extractor cone 10/10/100V, accelerating voltage into the collision cell 4V, ion transfer stage pressure $3.9/6.6/9.0 \times 10^{-3}\text{mbar}$, quadrupole analyzer pressure $9.0/9.1/9.5 \times 10^{-4}\text{mbar}$, ToF analyzer

pressure 1.7×10^{-6} mbar and 3.5×10^{-2} mbar of argon in the collision cell. For the tandem MS experiments, the quadrupole resolution was adjusted to encompass the entire charge state of interest, and spectra were acquired over a range of accelerating voltages into the collision cell. In-source dissociation of *MjHSP16.5* was accomplished by increasing the extractor cone voltage to 100V, and reducing the pressure in the ion transfer stage pressure to 1.8×10^{-3} mbar.

Surface Area Estimations

Estimating the surface area of the unfolded monomers released during CID was performed using three different methods.

- 1) The surface area of the folded monomers was determined by using SwissPDB DeepView software. An estimate of the surface area for an unfolded monomer was then determined by using a relationship between the sequence length and change in surface area upon unfolding [43].
- 2) An online utility (<http://roselab.jhu.edu/utis/unfolded.html>) which estimates lower and upper bounds for the surface area in the unfolded state, based both on an analysis of known structures and hard sphere Monte Carlo simulations [44, 45], was used.
- 3) Surface areas limits were also estimated by simple shape approximations: a sphere to model a globular protein, and a cylinder to model a completely extended polypeptide backbone. The predicted radius of the sphere was calculated from a relationship with the sequence length and radius of gyration of unfolded proteins [46]. The length of the cylinder was determined from the sequence length multiplied by the backbone length of an amino acid residue (3.57 \AA , from the average distance between adjacent α -carbons in the crystal structure). Its radius was estimated at 6.4 \AA from the average dimensions of the amino acids (weighted according to sequence).

The surface area for the *Ta*HSP16.9 12mer was estimated by approximating its structure to a cylinder of radius 47.5Å and height 55Å [30], while the structure of *Mj*HSP16.5 was approximated as a sphere of radius 60Å [31]. The surface areas of the stripped oligomers were estimated through scaling down the volumes of these shapes. These estimated surface areas match well within the limits imposed by calculations from charge-based estimations [38, 39].

The surface areas determined by these methods agree within approximately 15% of their average to each other, and therefore provide estimations adequately precise for the purpose of these studies.

REFERENCES

1. van den Heuvel, R.H., and Heck, A.J. (2004). Native protein mass spectrometry: from intact oligomers to functional machineries. *Curr Opin Chem Biol* 8, 519-526.
2. Benesch, J.L.P., and Robinson, C.V. (2006). Mass spectrometry of macromolecular assemblies: preservation and dissociation. *Curr Opin Struct Biol* *in press*.
3. Kennaway, C.K., Benesch, J.L.P., Gohlke, U., Wang, L., Robinson, C.V., Orlova, E.V., Saibil, H.R., and Keep, N.H. (2005). Dodecameric structure of the small heat shock protein Acr1 from *Mycobacterium tuberculosis*. *J Biol Chem.* 280, 33419-33425.
4. Rappas, M., Schumacher, J., Beuron, F., Niwa, H., Bordes, P., Wigneshwer, S., C.A., K., Robinson, C.V., Buck, M., and Zhang, X. (2005). Structural insights into the activity of enhancer-binding proteins. *Science* 307, 1972-1975.
5. Ilag, L.L., Videler, H., McKay, A.R., Sobott, F., Fucini, P., Nierhaus, K.H., and Robinson, C.V. (2005). Heptameric (L12)₆/L10 rather than canonical pentameric complexes are found by tandem MS of intact ribosomes from thermophilic bacteria. *Proc Natl Acad Sci U S A* 102, 8192-8197.
6. Aebersold, R., and Mann, M. (2003). Mass spectrometry-based proteomics. *Nature* 422, 198-207.
7. Thomas, J.J., Bothner, B., Traina, J., Benner, W.H., and Siuzdak, G. (2004). Electrospray ion mobility spectrometry of intact viruses. *Spectroscopy* 18, 31-36.
8. de la Mora, J.F. (2000). Electrospray ionization of large multiply charged species proceeds via Dole's charged residue mechanism. *Anal. Chim. Acta* 406, 93-104.
9. Sobott, F., and Robinson, C.V. (2004). Characterising electrosprayed biomolecules using tandem-MS - the noncovalent GroEL chaperonin assembly. *Int. J. Mass Spectrom.* 236, 25-32.

10. Jennings, K.R. (2000). The changing impact of the collision-induced decomposition of ions on mass spectrometry. *Int. J. Mass Spectrom.* *200*, 479-493.
11. Aquilina, J.A., Benesch, J.L.P., Bateman, O.A., Slingsby, C., and Robinson, C.V. (2003). Polydispersity of a mammalian chaperone: Mass spectrometry reveals the population of oligomers in α B-crystallin. *Proc. Natl. Acad. Sci. USA* *100*, 10611-10616.
12. Light-Wahl, K.J., Schwartz, B.L., and Smith, R.D. (1994). Observation of the noncovalent quaternary associations of proteins by electrospray ionization mass spectrometry. *J. Am. Chem. Soc.* *116*, 5271-5278.
13. Felitsyn, N., Kitova, E.N., and Klassen, J.S. (2001). Thermal decomposition of a gaseous multiprotein complex studied by blackbody infrared radiative dissociation. Investigating the origin of the asymmetric dissociation behavior. *Anal. Chem.* *73*, 4647-4661.
14. Felitsyn, N., Kitova, E.N., and Klassen, J.S. (2002). Thermal dissociation of the protein homodimer ecotin in the gas phase. *J. Am. Soc. Mass Spectrom.* *13*, 1432-1442.
15. Jurchen, J.C., and Williams, E.R. (2003). Origin of asymmetric charge partitioning in the dissociation of gas-phase protein homodimers. *J. Am. Chem. Soc.* *125*, 2817-2826.
16. Jurchen, J.C., Garcia, D.E., and Williams, E.R. (2004). Further studies on the origins of asymmetric charge partitioning in protein homodimers. *J. Am. Soc. Mass Spectrom.* *15*, 1408-1415.
17. Schwartz, B.L., Bruce, J.E., Anderson, G.A., Hofstadler, G.A., Rockwood, A.L., Smith, R.D., Chilkoti, A., and Stayton, P.S. (1995). Dissociation of tetrameric ions of noncovalent streptavidin complexes formed by electrospray ionization. *J. Am. Soc. Mass Spectrom.* *6*, 459-465.
18. Rostom, A.A., Sunde, M., Richardson, S.J., Schreiber, G., Jarvis, S., Bateman, R., Dobson, C.M., and Robinson, C.V. (1998). Dissection of multi-protein complexes using mass

spectrometry: subunit interactions in transthyretin and retinol-binding protein complexes.

Proteins Suppl 2, 3-11.

19. Sobott, F., McCammon, M.G., and Robinson, C.V. (2003). Gas-phase dissociation pathways of a tetrameric protein complex. *Int. J. Mass Spectrom.* 230, 193-200.
20. Versluis, C., van der Staaij, A., Stokvis, E., Heck, A.J., and de Craene, B. (2001). Metastable ion formation and disparate charge separation in the gas-phase dissection of protein assemblies studied by orthogonal time-of-flight mass spectrometry. *J. Am. Soc. Mass Spectrom.* 12, 329-336.
21. Versluis, C., and Heck, A.J.R. (2001). Gas-phase dissociation of hemoglobin. *Int. J. Mass Spectrom.* 210, 637-649.
22. Lei, Q.P., Cui, X., Kurtz, D.M., Jr., Amster, I.J., Chernushevich, I.V., and Standing, K.G. (1998). Electrospray mass spectrometry studies of non-heme iron-containing proteins. *Anal Chem* 70, 1838-1846.
23. Chernushevich, I.V., and Thomson, B.A. (2004). Collisional cooling of large ions in electrospray mass spectrometry. *Anal. Chem.* 76, 1754-1760.
24. McCammon, M.G., Hernandez, H., Sobott, F., and Robinson, C.V. (2004). Tandem mass spectrometry defines the stoichiometry and quaternary structural arrangement of tryptophan molecules in the multiprotein complex TRAP. *J. Am. Chem. Soc.* 126, 5950-5951.
25. Ilag, L.L., Ubarretxena-Belandia, I., Tate, C.G., and Robinson, C.V. (2004). Drug binding revealed by tandem mass spectrometry of a protein-micelle complex. *J Am Chem Soc* 126, 14362-14363.
26. Sharon, M., Witt, S., Felderer, K., Rockel, B., Baumeister, W., and Robinson, C.V. (2006). 20S proteasomes have the potential to keep substrates in store for continual degradation. *J Biol Chem.* *in press*

27. Aquilina, J.A., Benesch, J.L.P., Ding, L.L., Yaron, O., Horwitz, J., and Robinson, C.V. (2004). Phosphorylation of α B-crystallin alters chaperone function through loss of dimeric substructure. *J. Biol. Chem.* 279, 28675-28680.
28. Aquilina, J.A., Benesch, J.L.P., Ding, L.L., Yaron, O., Horwitz, J., and Robinson, C.V. (2005). Subunit exchange of polydisperse proteins: mass spectrometry reveals consequences of α A-crystallin truncation. *J Biol Chem* 280, 14485-14491.
29. van Duijn, E., Simmons, D.A., van den Heuvel, R.H.H., Bakkes, P.J., van Heerikhuizen, H., Heeren, R.M.A., Robinson, C.V., van der Vies, S.M., and Heck, A.J. (2006). Tandem Mass Spectrometry of Intact GroEL-Substrate Complexes Reveals Substrate-Specific Conformational Changes in the trans Ring. *J. Am. Chem. Soc.* *in press*
30. van Montfort, R.L., Basha, E., Friedrich, K.L., Slingsby, C., and Vierling, E. (2001). Crystal structure and assembly of a eukaryotic small heat shock protein. *Nat. Struct. Biol.* 8, 1025-1030.
31. Kim, K.K., Kim, R., and Kim, S.H. (1998). Crystal structure of a small heat-shock protein. *Nature* 394, 595-599.
32. Wilm, M., and Mann, M. (1996). Analytical properties of the nanoelectrospray ion source. *Anal. Chem.* 68, 1-8.
33. Benesch, J.L.P., Sobott, F., and Robinson, C.V. (2003). Thermal dissociation of multimeric protein complexes by using nanoelectrospray mass spectrometry. *Anal. Chem.* 75, 2208-2214.
34. van Montfort, R., Slingsby, C., and Vierling, E. (2002). Structure and function of the small heat shock protein/ α -crystallin family of molecular chaperones. *Adv. Protein Chem.* 59, 105-156.
35. Sobott, F., Benesch, J.L.P., Vierling, E., and Robinson, C.V. (2002). Subunit exchange of multimeric protein complexes: real-time monitoring of subunit exchange between small heat shock proteins by using electrospray-mass spectrometry. *J. Biol. Chem.* 277, 38921-38929.

36. Loo, J.A., Berhane, B., Kaddis, C.S., Wooding, K.M., Xie, Y., Kaufman, S.L., and Chernushevich, I.V. (2005). Electrospray ionization mass spectrometry and ion mobility analysis of the 20S proteasome complex. *J Am Soc Mass Spectrom* 16, 998-1008.
37. Csiszar, S., and Thachuk, M. (2004). Using ellipsoids to model charge distributions in gas phase protein complex ion dissociation. *Can. J. Chem.* 82, 1736-1744.
38. Kaltashov, I.A., and Mohimen, A. (2005). Estimates of protein surface areas in solution by electrospray ionization mass spectrometry. *Anal Chem* 77, 5370-5379.
39. Hauteux, M., Hue, N., de Kerdaniel, A.D., Zahir, A., Malec, V., and Laprévote, O. (2004). Under non-denaturing conditions, the mean charge state of a multiply charged protein formed by electrospray is linearly correlated with the macromolecular surface. *Int. J. Mass Spectrom.* 231, 131-137.
40. Keetch, C.A., Bromley, E.H., McCammon, M.G., Wang, N., Christodoulou, J., and Robinson, C.V. (2005). Leu55Pro transthyretin accelerates subunit exchange and leads to rapid formation of hybrid tetramers. *J Biol Chem.*
41. Bova, M.P., Huang, Q., Ding, L., and Horwitz, J. (2002). Subunit exchange, conformational stability, and chaperone-like function of the small heat shock protein 16.5 from *Methanococcus jannaschii*. *J. Biol. Chem.* 277, 38468-38475.
42. Sobott, F., Hernández, H., McCammon, M.G., Tito, M.A., and Robinson, C.V. (2002). A tandem mass spectrometer for improved transmission and analysis of large macromolecular assemblies. *Anal. Chem.* 74, 1402-1407.
43. Myers, J.K., Pace, C.N., and Scholtz, J.M. (1995). Denaturant m values and heat capacity changes: relation to changes in accessible surface areas of protein unfolding. *Protein Sci.* 4, 2138-2148.

44. Creamer, T.P., Srinivasan, R., and Rose, G.D. (1995). Modeling unfolded states of peptides and proteins. *Biochemistry* *34*, 16245-16250.
45. Creamer, T.P., Srinivasan, R., and Rose, G.D. (1997). Modeling unfolded states of proteins and peptides. II. Backbone solvent accessibility. *Biochemistry* *36*, 2832-2835.
46. Kohn, J.E., Millett, I.S., Jacob, J., Zagrovic, B., Dillon, T.M., Cingel, N., Dothager, R.S., Seifert, S., Thiyagarajan, P., Sosnick, T.R., Hasan, M.Z., Pande, V.S., Ruczinski, I., Doniach, S., and Plaxco, K.W. (2004). Random-coil behavior and the dimensions of chemically unfolded proteins. *Proc. Natl. Acad. Sci. USA* *101*, 12491-12496.

FIGURE AND TABLE LEGENDS

Figure 1: Nanoelectrospray mass spectra of *TaHSP16.9* and *MjHSP16.5*

Under non-dissociative conditions the mass of *TaHSP16.9*, **(A)**, was measured as 200790Da, corresponding to a 12-subunit oligomer, whereas *MjHSP16.5*, **(B)**, was observed as a 24-mer of 395107Da. These are both in agreement with the X-ray structures [30, 31]. The slight difference between the measured and sequence mass is attributed to residual binding of solvent molecules and buffer ions [9]. Inset are the crystal structures of the oligomeric proteins, depicting their equilibrium in solution with dimeric forms. *MjHSP16.5* can be dissociated, **(C)**, by increasing the extractor cone voltage from 10 to 100V while concurrently reducing the pressure in the ion transfer stage from 6.6×10^{-3} to 1.8×10^{-3} mbar (**upper panel**) or increasing the accelerating voltage into the collision cell from 4 to 100V (**lower panel**). Monomers (yellow), 23mers (blue) and 22mers (purple) are formed upon activation of the 24mers (green) in both cases, suggesting that the same dissociation mechanism applies to both methods of dissociation. The spectra are magnified 6-fold above 10000 m/z .

Figure 2: Dissociation of *TaHSP16.9*

(A) Dissociation of the 12mers results in the formation of highly-charged monomers at low m/z , and lowly charged 11mers at high m/z . At higher collision energies these, in turn, dissociate into monomers and 10mers. The spectrum is magnified 10-fold above 7500 m/z . Plotting the intensity of the 12mers (green circles), 11mers (blue triangles), and 10mers (purple squares), **(B)**, clearly shows the sequential nature of this multiple loss of subunits. This allows us to delineate a dissociation scheme, **(C)**, which shows the average charge states of the different species.

Figure 3: Dissociation of *Mj*HSP16.5

(A) A contour plot shows that the 24mers dissociate into highly charged monomers at low m/z , and lowly charged stripped 23, 22 and 21mers at high m/z . Monomers and oligomers are not shown on the same scale. Plotting the intensity of the 24mers (green circles), 23mers (blue triangles), 22mers (purple squares) and 21mers (red diamonds), (B), shows the sequential nature of this loss, similar to that observed for *Ta*HSP16.9. This enables us to delineate a dissociation scheme, (C), which shows the average charge states of the different species.

Figure 4: Dissociation of α B-crystallin

(A) In the MS spectrum of this protein the individual species that comprise its polydisperse assembly cannot be identified. Reprinted with permission from [11]. To overcome this, the peak corresponding to all the species, each carrying twice as many charges as subunits (marked *) is isolated and dissociated by CID [11], (B). The oligomers dissociate into highly charged monomers at low m/z , and lowly charged singly, doubly and triply stripped oligomers at high m/z . This spectrum is magnified 12-fold above 12000 m/z . (C), The dissociation pathway of one of these oligomeric sizes: 28mers (green circles) dissociate into 27mers (blue triangles), 26mers (purple squares), and 25mers (red diamonds).

Figure 5: Sub-oligomeric structure elucidations from dissociation pathways

A much larger initial kinetic energy (accelerating voltage \times charge state of the parent oligomer) difference between the maximum for the formation of singly (black) and doubly (white) stripped oligomers is observed for α B-crystallin (triangles) relative to *Mj*HSP16.5 (circles). This reflects the dimeric sub-structure observed in *Mj*HSP16.5 which is not present in the isolated α B-crystallin.

Figure 6: Chart demonstrating potential of tandem MS in structural biology.

Performing CID experiments leads to a number of experimental observables which can be subdivided into two categories: the CID products detected, or the dissociation process itself (inner segments, orange). These different observables lead to various levels of information, pertaining to both global and local structural organization (outer segments, blue).

Table 1: Partitioning of charge, mass and surface area upon dissociation

TaHSP16.9 (**upper**) and *MjHSP16.5* (**lower**). ^a The charge was determined from the average charge states of the stripped oligomers in figures 2/3A, averaged over all charge states. Monomer charge states were determined by subtracting the stripped oligomer charge state from its parent oligomer's charge state. ^b Percentage charge, mass, and surface area refers to the partitioning of each of these attributes that occurred during the dissociation event (e.g. 12mer → 11mer + monomer, or 11mer → 10mer + monomer). ^c The masses quoted are those determined from the spectra in figures 2/3 A. ^d Upper and lower bounds for the surface area of the unfolded monomers are the largest and smallest estimated by the different approaches detailed in the Experimental Procedures.

TABLE 1

<i>Ta</i> HSP16.9	12mer	11mer	Monomer	10mer	Monomer
Charge (z) ^a	32.0	17.4	14.6	10.4	7.0
Charge (%) ^b		54.4	45.6	59.8	40.2
Mass (Da) ^c	200948	184267	16726	167397	16726
Mass (%) ^b		91.7	8.3	90.8	9.1
Surface area (\AA^2) ^d	30591	29223	16708-23094	27855	16708-23094
Surface area (%) ^b		55.9-63.6	36.4-44.1	54.7-62.5	37.5-45.3

<i>Mj</i> HSP16.5	24mer	23mer	Monomer	22mer	Monomer	21mer	Monomer
Charge (z) ^a	47.0	33.4	13.6	22.0	11.4	15.6	6.4
Charge (%) ^b		71.0	29.0	65.9	34.1	70.7	29.3
Mass (Da) ^c	395107	378852	16452	362241	16452	345721	16452
Mass (%) ^b		95.9	4.2	95.6	4.3	95.4	4.5
Surface area (\AA^2) ^d	45239	43966	16316-21360	42682	16316-21360	41374	16316-21360
Surface area (%) ^b		67.3-72.9	27.1-32.7	66.7-72.3	27.7-33.3	66.0-71.7	28.3-34.1

FIGURE 1

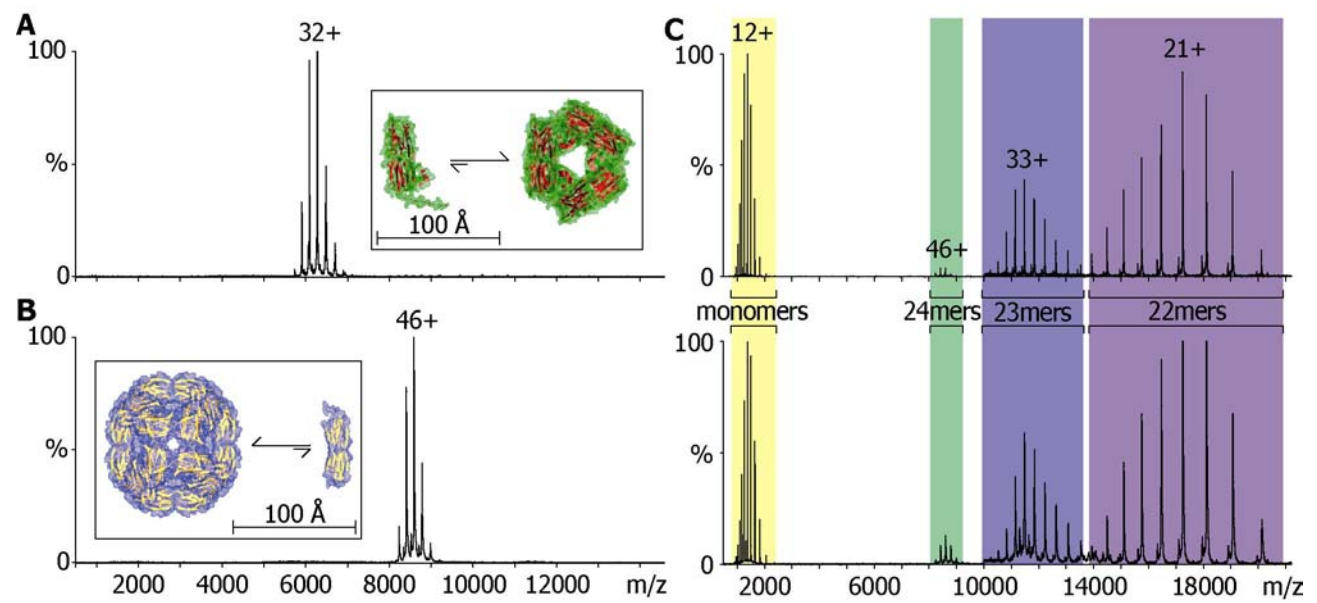


FIGURE 2

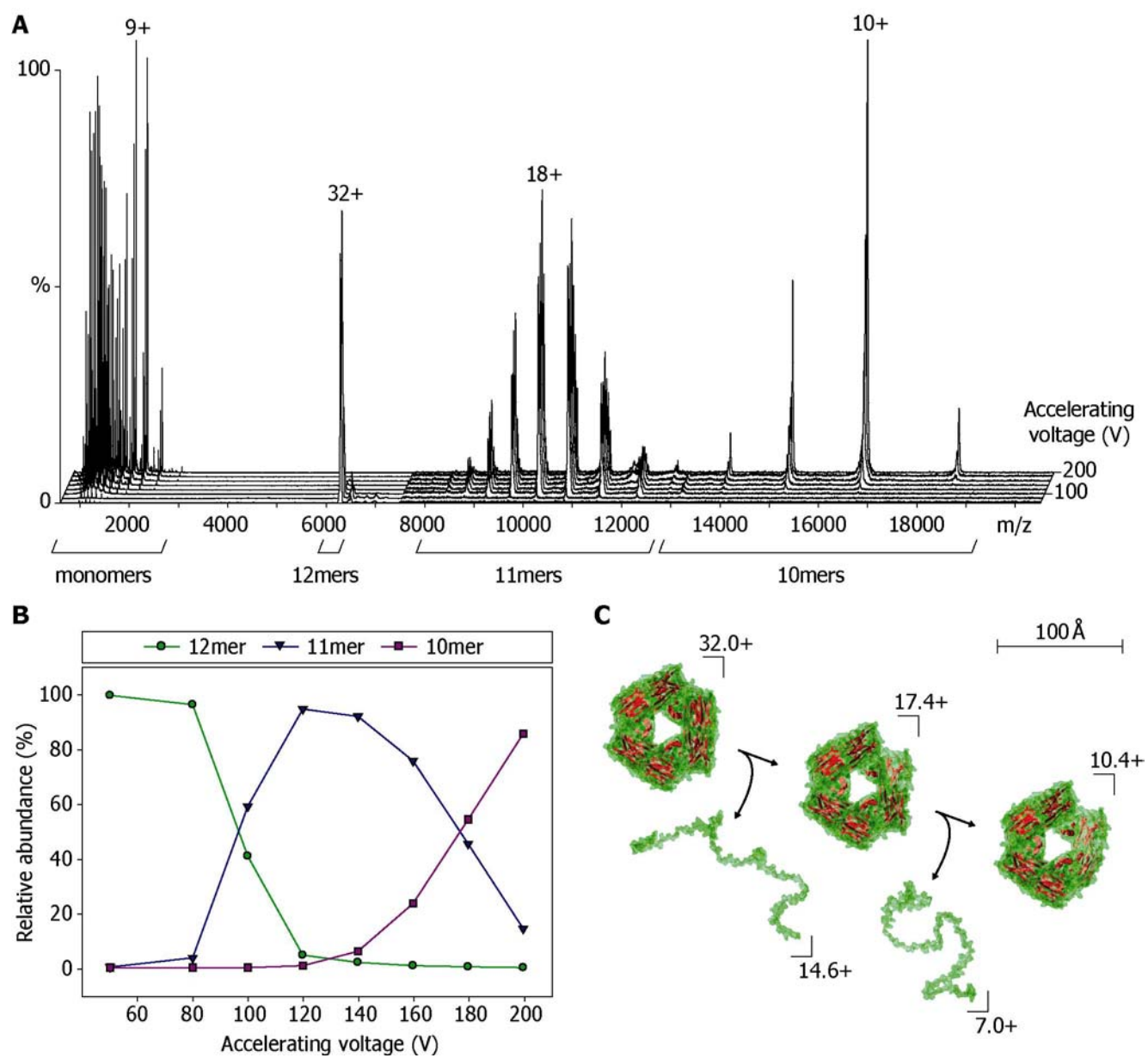


FIGURE 3

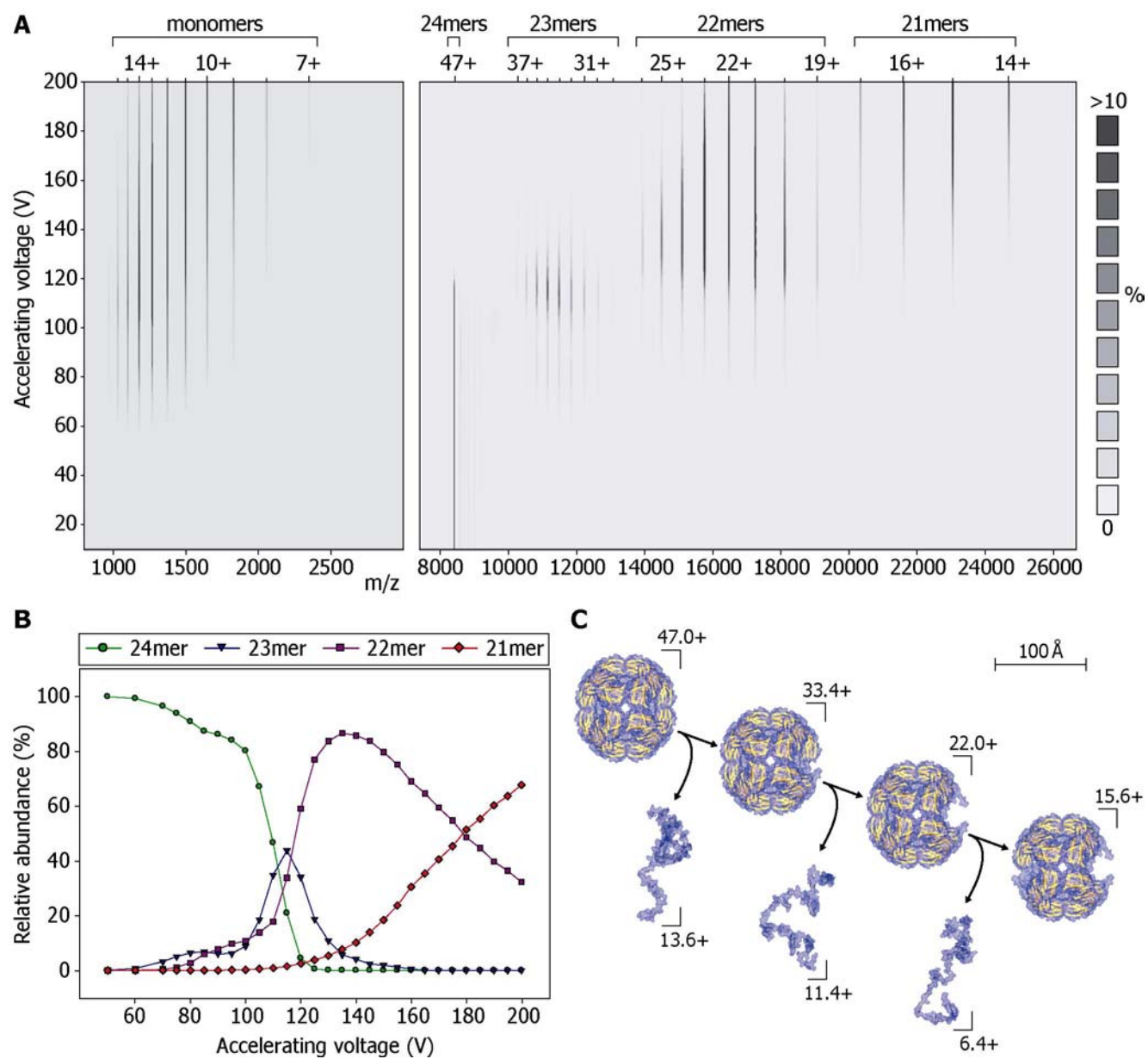


FIGURE 4

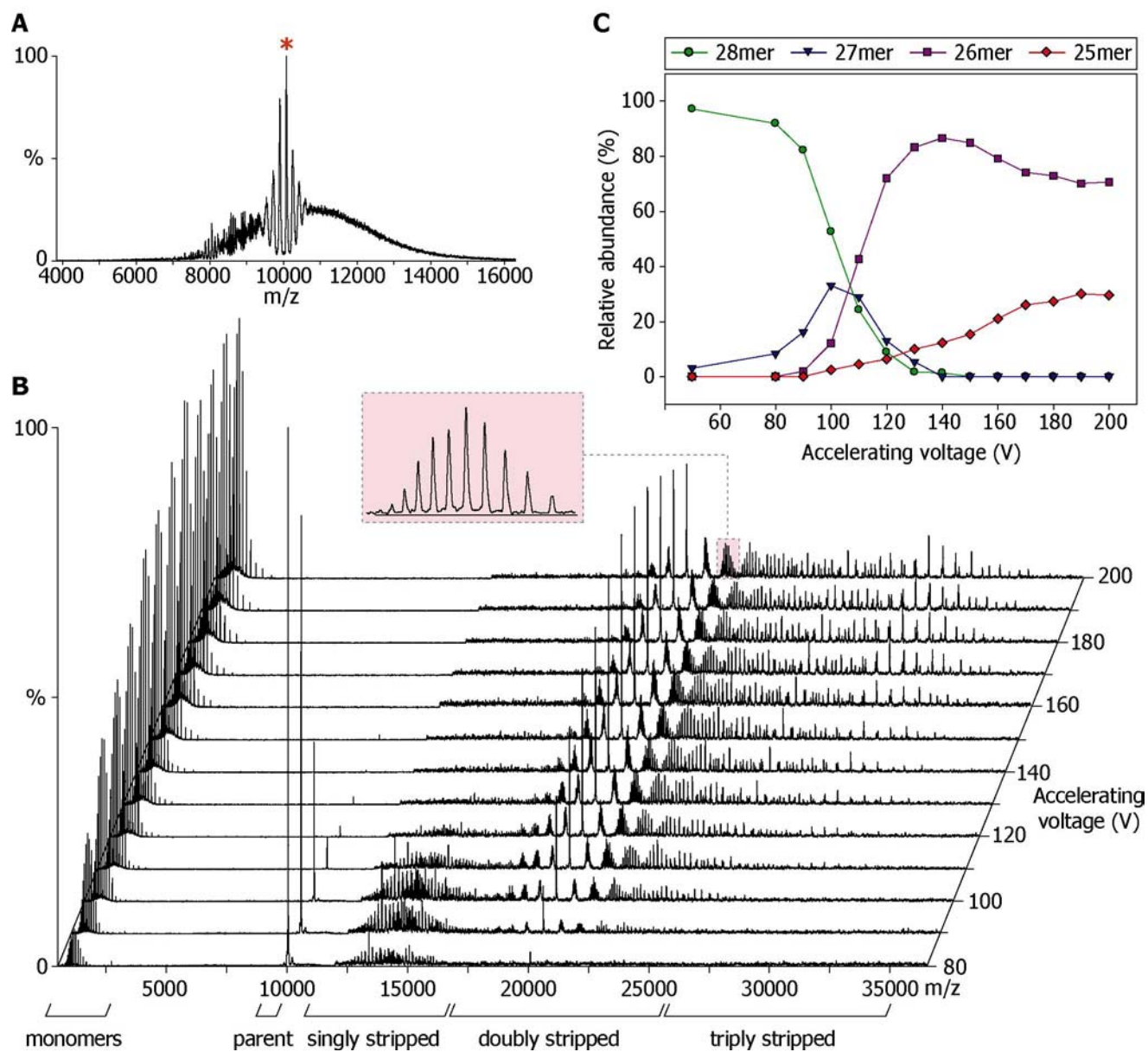


FIGURE 5

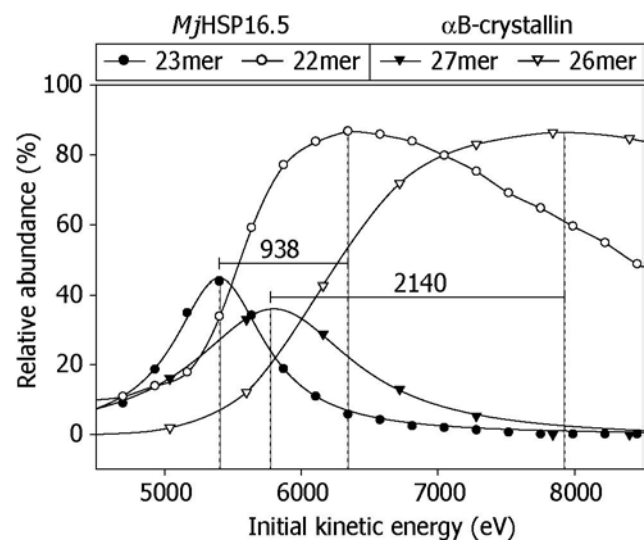


FIGURE 6

